

Contribution No. 5212 from the Central Research and Development Department, Experimental Station E328, E. I. du Pont de Nemours and Company, Wilmington, Delaware 19880-0328, and Contribution from the Department of Chemistry, Northeastern University, Boston, Massachusetts 02115

Structural and Magnetic Characterization of Electron-Transfer Salts of Hexacyanotrimethylenecyclopropanide, $[C_3[C(CN)_2]_3]^{3-}$ and $[Fe(C_5Me_5)_2]^{2+}$ (1:1; Two Phases) and $[Fe(C_6H_3Me_3)_2]^{2+}$ (1:2). Evidence for 1-D Antiferromagnetic Behavior in Segregated $[Fe(C_5Me_5)_2]^{2+}$ Chains

Joel S. Miller,^{*1a} Michael D. Ward,^{*1a,c} Jian H. Zhang,^{1b} and William M. Reiff^{*1b}

Received November 27, 1989

The reaction of $S = 1/2$ hexacyanotrimethylenecyclopropanide, $[C_3[C(CN)_2]_3]^{3-}$, acceptors (A^-) with organometallic cation donors (D^{2+}) results in the formation of extended linear chain compounds. Reaction of A^- with $[Fe(C_5Me_5)_2]^{2+}$ results in the formation of at least two 1:1 phases of $[Fe(C_5Me_5)_2]^{2+}[C_3[C(CN)_2]_3]^{3-}$, and reaction with $[Fe(C_6Me_3H_3)_2]^{2+}$ leads to the 1:2 phase $[Fe(C_6Me_3H_3)_2]^{2+}[C_3[C(CN)_2]_3]^{3-}$. One of the 1:1 phases crystallizes in the centrosymmetric monoclinic $C2/c$ space group [$a = 15.207$ (3) Å, $b = 26.500$ (6) Å, $c = 7.287$ (4) Å, $\beta = 107.46$ (3)°, $Z = 4$, $V = 2801.2$ Å³, $T = -108$ °C, $R(F_o^2) = 0.053$, $R_w(F_o^2) = 0.056$] and possesses segregated $\cdots D^{2+} D^{2+} D^{2+} \cdots$ and $\cdots A^- A^- A^- \cdots$ 1-D chains of $S = 1/2$ cations and $S = 1/2$ anions. The anions are canted 28.75° with respect to the c axis and exhibit uniform spacings of 3.224 Å between the planes of the anions. The shortest interchain $Fe^{III}\cdots Fe^{III}$ distance is 7.287 Å, whereas the shortest intrachain $Fe\cdots Fe$ distance is 8.701 Å. The second 1:1 polymorph crystallizes in the triclinic $P\bar{1}$ space group [$a = 7.532$ (7) Å, $b = 14.776$ (6) Å, $c = 14.981$ (6) Å, $\alpha = 115.90$ (4)°, $\beta = 95.76$ (6)°, $\gamma = 101.74$ (5)°, $Z = 2$, and $V = 1442$ Å³ at room temperature] and is isomorphous with $[Co(C_5Me_5)_2]^{2+}[C_3[C(CN)_2]_3]^{3-}$ [$a = 7.421$ (5) Å, $b = 14.763$ (7) Å, $c = 14.969$ (6) Å, $\alpha = 115.90$ (3)°, $\beta = 96.02$ (4)°, $\gamma = 101.22$ (4)°, $V = 1413$ (3) Å³, $R(F_o^2) = 0.065$, $R_w(F_o^2) = 0.063$ at -40 °C], which possesses $\cdots D^{2+} D^{2+} D^{2+} \cdots$ and $\cdots A^- A^- A^- \cdots$ segregated chains of $S = 1/2$ cations and $S = 1/2$ anions. Both the cations and anions form chains parallel to a . The anions exhibit uniform spacing of 3.20 Å between planes of the anions. The 1:2 $[Fe(C_6Me_3H_3)_2]^{2+}[C_3[C(CN)_2]_3]^{3-}$ phase crystallizes in the triclinic $P\bar{1}$ space group [$a = 9.156$ (2) Å, $b = 9.171$ (2) Å, $c = 11.523$ (3) Å, $\alpha = 77.92$ (2)°, $\beta = 80.20$ (2)°, $\gamma = 81.31$ (2)°, $V = 925.7$ (8) Å³, $Z = 1$, $R(F_o^2) = 0.077$, $R_w(F_o^2) = 0.092$ at -91 °C]. This complex exhibits segregated chains of $S = 0$ dications and $S = 0$ dimer dianions, but also has unusual $\cdots D^{2+} A_2^{2-} D^{2+} A_2^{2-} \cdots$ mixed-stack linear chains in which the anion planes are nearly perpendicular to the C_6 ligand rings. This motif results in intermolecular contact distances between the cyano nitrogen atoms of the $[C_3[C(CN)_2]_3]^{3-}$ dimer pair and the ring carbons of the $[Fe(C_6Me_3H_3)_2]^{2+}$ cation that are less than the sum of the van der Waals radii. The planar $S = 1/2$ anion has average ring C—C, ring—C(CN)₂, C—CN, and C≡N distances of 1.385, 1.383, 1.437, and 1.126 Å, respectively, and ring—C—CN and NC—C—CN angles of 120.6 and 118.9°, respectively. The corrected molar magnetic susceptibilities of the 1:1 monoclinic and triclinic phases obey the Curie-Weiss expression, $\chi = C/(T - \theta)$, with $\theta = -3.4$ K and $\mu_{eff} = 2.98 \mu_B$ and $\theta = -3.4$ K and $\mu_{eff} = 3.10 \mu_B$, respectively. Above 78 K, each of the $[Fe(C_5Me_5)_2]^{2+}$ polymorphs exhibit classical singlet ⁵⁷Fe Mössbauer spectra typical of the low-spin Fe(III) cation. For the monoclinic phase, the 0.36 K spectrum indicates a magnetic hyperfine splitting, H_n , of 455 kG. For the triclinic polymorph H_n is 431 kG at 4.68. The Mössbauer spectra are consistent with slow paramagnetic relaxation extending to unusually high temperatures as opposed to an onset of 3-D magnetic ordering. The magnetization data for the monoclinic phase indicate that the anion chain is diamagnetic, i.e., it exhibits strong antiferromagnetic coupling. Below 40 K in a field of 30 G, the susceptibility for this phase exhibits a broad maximum at ~4 K consistent with a Bonner-Fisher type of 1-D antiferromagnetic exchange interaction, which is attributed to 1-D antiferromagnetic coupling along the cation chains. However, applied fields greater than 100 G result in decoupling of the weak intrachain-cation antiferromagnetic magnetic interaction, inducing an essentially complete transformation to a higher moment state. For $[Fe(C_6Me_3H_3)_2]^{2+}[C_3[C(CN)_2]_3]^{3-}$, magnetic susceptibility and EPR studies indicate the presence of a thermally populated triplet state 0.11 eV (890 cm⁻¹, 1280 K, 2.56 kcal/mol) above the ground state that is associated with the dimer dianions.

Introduction

The investigation of one-dimensional (1-D) electron-transfer complexes has resulted in the discovery of numerous interesting electronic properties in these materials.²⁻⁵ For example, cooperative meta magnetic behavior was observed^{6,7} in the 1-D phase of $[Fe(C_5Me_5)_2]^{2+}[TCNQ]^-$ ($TCNQ = 7,7,8,8$ -tetracyano-*p*-quinodimethane). Bulk ferromagnetism in $[Fe(C_5Me_5)_2]^{2+}[TCNE]^-$ ($TCNE =$ tetracyanoethene) was demonstrated by a spontaneous magnetic moment at zero applied field.⁸⁻¹¹ With

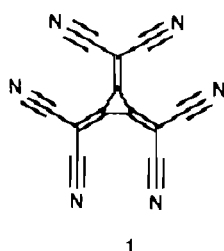
these observations of meta- and ferromagnetic behavior in 1-D electron-transfer complexes, the systematic study of the structure-function relationships of electron-transfer solids comprising metallocenium cations and planar polycyanoanions in an alternate mixed stack motif ($\cdots D^{2+} A^- D^{2+} A^- \cdots$) was undertaken with the goal of elucidating the electronic and steric requirements for the stabilization of the ferromagnetic state in molecular materials.^{9,11-17}

- (1) (a) E. I. du Pont de Nemours and Company, Inc. (b) Northeastern University. (c) Current address: Department of Chemical Engineering, University of Minnesota, Minneapolis, MN 55455.
- (2) Simon, J.; André, J. J. *Molecular Semiconductors*; Springer Verlag: New York, 1985.
- (3) Epstein, A. J.; Miller, J. S. *Sci. Am.* **1979**, *240* (4), 52-61. Bechgaard, K.; Jerome, D. *Sci. Am.* **1982**, *247* (2), 52-61.
- (4) Miller, J. S., Ed.; *Extended Linear Chain Compounds*; Plenum Publishing Corp.: New York, 1982, Vols. 1 and 2; 1983, Vol. 3.
- (5) For a detailed overview, see the proceedings of the recent series of international conferences: *Syn. Met.* **1988**, *27*; **1989**, *28* (3), 29 (1, 2, and 4). *Mol. Cryst. Liq. Cryst.* **1985**, *117-121*. *J. Phys. Colloq.* **1983**, *44-C3*. *Mol. Cryst. Liq. Cryst.* **1981**, *77*, *79*, *82*, *83*, *85*; **1982**, *86*. *Chem. Scr.* **1981**, *17*. *Lect. Notes Phys.* **1979**, *95*, *96*. *Ann. N.Y. Acad. Sci.* **1978**, *313*.
- (6) Candela, G. A.; Swarzenruber, L.; Miller, J. S.; Rice, M. J. *J. Am. Chem. Soc.* **1979**, *101*, 2755-2756.
- (7) Stryjewski, E.; Giordano, N. *Adv. Phys.* **1977**, *26*, 487-650.
- (8) Miller, J. S.; Calabrese, J. C.; Bigelow, R. W.; Epstein, A. J.; Zhang, J. H.; Chittipeddi, S.; Reiff, W. M. *Chem. Commun.* **1986**, 1026-1028.

- (9) Miller, J. S.; Calabrese, J. C.; Epstein, A. J.; Bigelow, R. W.; Reiff, W. M.; Zhang, J. H. *J. Am. Chem. Soc.* **1987**, *109*, 769-781.
- (10) Chittipeddi, S.; Kromack, K. R.; Miller, J. S.; Epstein, A. J. *J. Phys. Rev. Lett.* **1987**, *22*, 2695.
- (11) Miller, J. S.; Epstein, A. J.; Reiff, W. M. *Acc. Chem. Res.* **1988**, *21*, 114-120. Miller, J. S.; Epstein, A. J.; Reiff, W. M. *Science* **1988**, *240*, 40-47. Miller, J. S.; Epstein, A. J.; Reiff, W. M. *Chem. Rev.* **1988**, *88*, 201-220. Miller, J. S.; Epstein, A. J. *New Aspects of Organic Chemistry*; Yoshida, Z., Shiba, T., Ohsiro, Y., Eds.; VCH Publishers: New York, 1989; p 237.
- (12) Dixon, D. A.; Calabrese, J. C.; Miller, J. S. *J. Am. Chem. Soc.* **1986**, *108*, 2582-2588.
- (13) Miller, J. S.; Zhang, J. H.; Reiff, W. M.; Preston, L. D.; Reis, A. H., Jr.; Gebert, E.; Extine, M.; Troup, J.; Dixon, D. A.; Epstein, A. J.; Ward, M. D. *J. Phys. Chem.* **1987**, *91*, 4344.
- (14) (a) Zhang, J. H.; Reiff, W. M.; Calabrese, J. C.; Miller, J. S. Manuscript in preparation. (b) Zhang, J. H.; Reiff, W. M.; Miller, J. S. Manuscript in preparation.
- (15) (a) Gebert, E.; Reis, A. H., Jr.; Miller, J. S.; Rommelmann, H.; Epstein, A. J. *J. Am. Chem. Soc.* **1982**, *104*, 4403-4410. (b) Miller, J. S.; Krusic, P. J.; Dixon, D. A.; Reiff, W. M.; Zhang, J. H.; Anderson, E. C.; Epstein, A. J. *J. Am. Chem. Soc.* **1986**, *108*, 4459-4466.

The McConnell mechanism^{11,18,20} suggested that electron-transfer salts with this structure type could stabilize ferromagnetic coupling provided that cations or anions with thermally accessible triplet states are utilized.^{11,18}

Although many salts containing cyanocarbon anions have been investigated, those containing the D_{3h} hexacyanotrimethylene-cyclopropane monoanion, $[C_3[C(CN)_2]_3]^{1-}$ (**1**)^{21,22} have not been



1

reported extensively. The monoanion has been proposed as a component for ferromagnetic molecular solids.^{19c} Recently, an electron-transfer complex with an organic cation was reported^{19d} to exhibit antiferromagnetic behavior, but the lack of structural information precluded further understanding of the magnetic properties. More detailed structural information was reported recently for organometallic salts of **1**.²³ In an effort to elucidate further the properties of electron-transfer complexes containing **1** that exhibit antiferromagnetic behavior, we have prepared and investigated some organometallic electron-transfer salts. Herein we report the preparation, structure, and physical properties of $[C_3[C(CN)_2]_3]^{1-}$ in electron-transfer complexes with $[Fe(C_5Me_5)_2]^{2+}$ and $[Fe(C_6Me_6H_3)_2]^{2+}$.

Experimental Section

Acetonitrile was distilled from P_2O_5 and subsequently CaH_2 under nitrogen, and nitromethane was distilled from $CaSO_4$ under nitrogen. Tetra-*n*-butylammonium tetrafluoroborate was recrystallized from ethyl acetate-ethanol and dried in vacuo prior to use. Literature methods were used for the preparation of $[Fe(C_6Me_6H_3)_2][PF_6]_2$,²⁴ $[Fe(C_5Me_5)_2][BF_4]$,⁹ $K[C_3[C(CN)_2]_3]$,^{22a} and $[n-Bu_4N][C_3[C(CN)_2]_3]$.^{22a} All manipulations were performed under inert-atmosphere conditions by using purified nitrogen and a Vacuum Atmospheres glovebox.

$[Fe(C_6Me_6H_3)_2][C_3[C(CN)_2]_3]$ was prepared at 10 °C by slow diffusion of diethyl ether into an open vial containing $[Fe(C_6Me_6H_3)_2][PF_6]_2$ (45 mg; 0.075 mmol) and $[n-Bu_4N][C_3[C(CN)_2]_3]$ (70 mg; 0.150 mmol) in 8 mL of acetonitrile. After 1 week, 23 mg (31%) of product was isolated by vacuum filtration as bronze, platelike crystals. Infrared spectra (Nujol): $\nu(C\equiv N) = 2207$ s, 2196 w, 2190 s, 2171 w cm^{-1} . These absorptions are in the range that are characteristic of $[C_3[C(CN)_2]_3]^{1-}$.^{22,25}

Monoclinic $[Fe(C_5Me_5)_2][C_3[C(CN)_2]_3]^{1-}$ (1:1) was prepared in an inert-atmosphere glovebox via reaction of $[Fe(C_5Me_5)_2][BF_4]$ (105 mg; 0.24 mmol) dissolved in 5 mL of acetonitrile with 120 mg (0.255 mmol) of $[n-Bu_4N][C_3[C(CN)_2]_3]$ dissolved in 30 mL of warm MeCN. After the volume was reduced to 30 mL, the solution was slowly cooled

Table I. Summary of Crystallographic Data for $[C_3[C(CN)_2]_3]^{1-}$ Salts of $[Fe(C_5Me_5)_2]^{2+}$ and $[Fe(C_6H_3Me_3)_2]^{2+}$

cation	$[Fe(C_5Me_5)_2]^{2+}$	$[Co(C_5Me_5)_2]^{2+}$	$[Fe(C_6H_3Me_3)_2]^{2+}$
anion	$[C_3[C(CN)_2]_3]^{1-}$	$[C_3[C(CN)_2]_3]^{1-}$	$[C_3[C(CN)_2]_3]^{1-}$
cation:anion	1:1	1:1	1:2
formula	$C_{32}H_{30}FeN_6$	$C_{32}H_{30}CoN_6$	$C_{42}H_{24}FeN_{12}$
mol wt	554.48	557.57	752.39
radiation; λ , Å	Mo K α ; 0.710 73	Cu K α ; 1.541 84	Mo K α ; 0.710 73
temp, °C	-108 ± 1	-40 ± 1	-91 ± 1
space group	$C2/c$	$P\bar{1}$	$P\bar{1}$
no.	15	2	2
<i>a</i> , Å	15.207 (3)	7.421 (5)	9.156 (2)
<i>b</i> , Å	26.500 (6)	14.763 (7)	9.171 (2)
<i>c</i> , Å	7.287 (4)	14.696 (6)	11.523 (3)
α , deg	90.	115.90 (3)	77.92 (2)
β , deg	107.46 (3)	96.02 (4)	80.20 (2)
γ , deg	90.	101.22 (4)	81.31 (2)
<i>V</i> , Å ³	2801.2	1413 (3)	925.7 (8)
<i>Z</i>	4	2	1
density, g/cm ³	1.31	1.31	1.35
μ , cm ⁻¹	5.9	52.1	4.72
$R(F_o^2)$	0.053	0.065	0.077
$R_w(F_o^2)$	0.056	0.063	0.092

to room temperature and 93 mg of the purple-black product (0.168 mmol; 66%) was collected via vacuum filtration. Anal. Calcd for $C_{32}H_{30}FeN_6$: C, 69.32; H, 5.45; Fe, 10.07; N, 15.16. Found: C, 69.31; H, 5.22; N, 15.79. Infrared spectra (Nujol): $\nu(C\equiv N) = 2196$ m, 2210 s cm^{-1} . These absorptions are characteristic of $[C_3[C(CN)_2]_3]^{1-}$.^{22,25} Crystals recrystallized from 1,2-dichloroethane were used for single-crystal X-ray diffraction.

Triclinic $[Fe(C_5Me_5)_2][C_3[C(CN)_2]_3]^{1-}$ (1:1) was prepared from the reaction of $[Fe(C_5Me_5)_2][BF_4]$ (150 mg; 0.363 mmol) and $[n-Bu_4N][C_3[C(CN)_2]_3]$ (170 mg; 0.363 mmol), each dissolved in 5 mL of MeCN. Purple-black needle crystals of the product separated and were collected via vacuum filtration (149 mg; 0.26 mmol; 74%). After the volume was reduced to 3 mL, the solution was slowly cooled to -30 °C overnight, yielding 93 mg of product (0.168 mmol; 66%) after collection by vacuum filtration. Anal. Calcd for $C_{32}H_{30}FeN_6$: C, 69.32; H, 5.45; Fe, 10.07; N, 15.16. Found: C, 69.22; H, 5.49; N, 15.16. Infrared spectra (Nujol): $\nu(C\equiv N) = 2196$ w, 2210 s cm^{-1} . These absorptions are characteristic of $[C_3[C(CN)_2]_3]^{1-}$.^{22,25} Single-crystal X-ray diffraction studies indicated the centrosymmetric $P\bar{1}$ space group [$a = 7.532$ (7) Å, $b = 14.776$ (6) Å, $c = 14.981$ (6) Å, $\alpha = 115.90$ (4)°, $\beta = 95.76$ (6)°, $\gamma = 101.74$ (6)°, $V = 1442$ Å³]. This phase is isomorphous with the Co^{III} analogue (vide infra). Because the only difference between the Co^{III} and Fe^{III} complexes is the identity of the metal atoms, which have similar radii, the crystal structures are presumed to be identical.

Triclinic $[Co(C_5Me_5)_2][C_3[C(CN)_2]_3]^{1-}$ (1:1) was prepared from solutions containing $[Co(C_5Me_5)_2][PF_6]$ (Strem) (128 mg; 0.270 mmol; 1 mL of MeCN) and $[n-Bu_4N][C_3[C(CN)_2]_3]$ (127 mg; 0.270 mmol; 2 mL of MeCN). After mixing, the solution was refrigerated at -25 °C overnight, and 78 mg of the blue product (52%) was collected by vacuum filtration. Anal. Calcd for $C_{32}H_{30}CoN_6$: C, 68.93; H, 5.42; N, 15.08. Found: C, 69.07; H, 5.79; N, 14.57. Infrared spectra (Nujol): $\nu(C\equiv N) = 2196$ m, 2210 s cm^{-1} . These absorptions are characteristic of $[C_3[C(CN)_2]_3]^{1-}$.^{22,25}

X-ray Data Collection, Reduction, Solution, and Refinement. Crystals of monoclinic $[Fe(C_5Me_5)_2][C_3[C(CN)_2]_3]$,^{26a} triclinic $[Co(C_5Me_5)_2][C_3[C(CN)_2]_3]$,^{26b} and $[Fe(C_6Me_6H_3)_2][C_3[C(CN)_2]_3]_2$ were used to determine the single-crystal X-ray structures in the usual fashion.²⁷ The key parameters for the data collection, data reduction, solution, and refinement are summarized in Table I and described in detail in Table S1. The anisotropic thermal parameters, general displacement parameter, cation bond angles, and torsional angles as well as weighted least-

- (16) Miller, J. S.; Zhang, J. H.; Reiff, W. M. *J. Am. Chem. Soc.* **1987**, *109*, 4584.
- (17) Miller, J. S.; Calabrese, J. C.; Harlow, R. L.; Dixon, D. A.; Zhang, J. H.; Reiff, W. M.; Chittipeddi, S.; Selover, M. A.; Epstein, A. J. *J. Am. Chem. Soc.* **1990**, *112*, 5496.
- (18) McConnell, H. M. *Proc. Robert A. Welch Found. Conf. Chem. Res.* **1967**, *11*, 144.
- (19) (a) Breslow, R. *Pure Appl. Chem.* **1982**, *54*, 927-928. (b) Breslow, R.; Jaun, B.; Kluttz, R. Q.; Xia, C.-Z. *Tetrahedron* **1982**, *38*, 863-867. (c) Breslow, R. *Mol. Cryst. Liq. Cryst.* **1985**, *125*, 261-267. (d) LePage, T. J.; Breslow, R. *J. Am. Chem. Soc.* **1987**, *109*, 6412.
- (20) Miller, J. S.; Epstein, A. J. *J. Am. Chem. Soc.* **1987**, *109*, 3850.
- (21) Abrahams, S. C.; Bair, H. E.; DiSalvo, F. J.; Marsh, P.; Devring, L. A. *Phys. Rev. B* **1984**, *29*, 1258.
- (22) (a) Fukunaga, T. *J. Am. Chem. Soc.* **1976**, *98*, 610. (b) Fukunaga, T.; Gordon, M. D.; Krusic, P. J. *J. Am. Chem. Soc.* **1976**, *98*, 611; U.S. Patent 3,963,769, 1976.
- (23) Ward, M. D.; Fagan, P. J.; Calabrese, J. C.; Johnson, D. C. *J. Am. Chem. Soc.* **1989**, *111*, 1719.
- (24) Helling, J. F.; Braitsch, D. M. *J. Am. Chem. Soc.* **1970**, *92*, 7207.
- (25) Miller, J. S.; Dixon, D. A. *Science* **1987**, *235*, 871-873.

- (26) (a) Molecular Structure Corp. All calculations were performed on a PDP-11/60-based TEXRAY system, which includes the Enraf-Nonius SDP and proprietary crystallographic software of Molecular Structure Corp. (b) Onieda Research Services, Inc., Whitesboro, NY 13492.
- (27) A few crystals of a third 1:1 hexagonal phase have been sporadically isolated and characterized by X-ray diffraction [$a = b = 14.841$ (5) Å, $c = 10.676$ (2) Å, $\alpha = \beta = 90^\circ$, $\gamma = 120^\circ$, $V = 2036.4$ Å³, $T = -100$ °C]. Although the crystal did not diffract well enough for a complete refinement (only 173 observed reflections) a highly disordered ... D⁺A⁻D⁺A⁻... along *c* (i.e., the intrachain Fe...Fe distance is 10.676 Å, whereas the interchain Fe...Fe distances are 7.609, 9.774, 12.662, and 18.714 Å).

Table II. Positional Parameters and Their Estimated Standard Deviations for 1:1 Monoclinic $[\text{Fe}(\text{C}_5\text{Me}_5)_2]^{+}[\text{C}_3[\text{C}(\text{CN})_2]_3]^{-}$

atom	x	y	z
Fe	0.0000	0.16303 (5)	0.2500
N1	0.1296 (4)	0.3861 (2)	0.4877 (8)
N2	-0.1253 (4)	0.6557 (2)	0.0497 (8)
N3	-0.2482 (4)	0.5103 (2)	-0.1760 (8)
C1	0.0806 (4)	0.1651 (3)	0.5378 (8)
C2	0.0208 (4)	0.2071 (2)	0.4978 (9)
C3	-0.0711 (4)	0.1889 (2)	0.4367 (8)
C4	-0.0683 (4)	0.1348 (2)	0.4406 (9)
C5	0.0268 (4)	0.1203 (2)	0.5008 (9)
C6	0.1839 (4)	0.1655 (3)	0.6112 (9)
C7	0.0500 (5)	0.2611 (3)	0.5210 (11)
C8	-0.1562 (4)	0.2202 (3)	0.3871 (10)
C9	-0.1484 (4)	0.1007 (2)	0.3921 (10)
C10	0.0617 (5)	0.0670 (3)	0.5265 (10)
C11	0.0735 (4)	0.4084 (2)	0.3832 (9)
C12	0.0000	0.4630 (3)	0.2500 (0)
C13	0.0000	0.4881 (3)	0.2500 (0)
C14	-0.0422 (4)	0.5337 (2)	0.1805 (8)
C15	-0.1155 (4)	0.5591 (2)	0.0558 (8)
C16	-0.1192 (4)	0.6135 (3)	0.0550 (9)
C17	-0.1898 (4)	0.5317 (2)	-0.0720 (9)

squares planes are included as supplementary material. Scattering factors were taken from Cromer and Waber.^{28a} Anomalous dispersion effects were included in F_o ; the values for $\Delta f'$ and $\Delta f''$ where those of Cromer.^{28c}

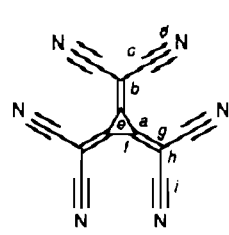
⁵⁷Fe Mössbauer Spectra. Zero-field Mössbauer spectra between 1.6 and 300 K were determined by using a conventional constant acceleration spectrometer with a 50-mCi ⁵⁷Co source electroplated onto the surface and annealed into the body of a 6- μm -thick foil of high-purity rhodium in a hydrogen atmosphere. The details of cryogenics, temperature control, etc have been described previously.^{29a} The Mössbauer spectra below 1.6 K for the monoclinic polymorph were obtained in a closed-cycle carbon sorption pumped ³He cryostat.³⁰

Magnetic Measurements. The magnetic susceptibility was determined for powder samples over the 1.66–5.10-kG applied field range by using a Faraday balance as previously described.²⁹ Additional very low-field (30 G) susceptibility and field dependence of magnetization were determined by using the SHE "SQUID" magnetometer at the Francis Bitter National Magnet Laboratory. On the basis of magnet history, the remnant field has been estimated to be as high as 10 G.

Spectroscopic Measurements. Infrared spectra were recorded on a Nicolet 7199 Fourier-transform spectrometer. The UV-visible spectra were recorded on a Cary 2390 spectrometer. The EPR spectra were recorded on an IBM/Bruker ER 200 D-SRC spectrometer.

Results and Discussion

Structural Characterization. 1:1 Monoclinic $[\text{Fe}(\text{C}_5\text{Me}_5)_2][\text{C}_3[\text{C}(\text{CN})_2]_3]$. The monoclinic unit cell comprises a half-cation and a half-anion. The atomic coordinates are presented in Table II. The $[\text{Fe}(\text{C}_5\text{Me}_5)_2]^{+}$ cation has local D_{5d} symmetry with Fe–C, C–C, and C–Me bond lengths ranging from 2.083 (8) to 2.106 (7), Å, from 1.412 (9) to 1.435 (8) Å, and from 1.473 (9) to 1.502 (10) Å, and averaging 2.092, 1.423, and 1.491 Å, respectively, which are in excellent agreement with values previously reported.⁹ The Fe...C₅ ring centroid distance is 1.706 Å and is comparable to those previously reported.⁹ The $[\text{C}_3[\text{C}(\text{CN})_2]_3]^{-}$

Table III. Average Chemically Equivalent Bond Distances (Å) and Angles (deg) for $[\text{C}_3[\text{C}(\text{CN})_2]_3]^{-}$


$[\text{Fe}(\text{C}_5\text{Me}_5)_2][\text{C}_3[\text{C}(\text{CN})_2]_3]$				
distance/angle	monoclinic phase	triclinic phase	$[\text{Fe}(\text{C}_6\text{H}_3\text{Me}_3)_2][\text{C}_3[\text{C}(\text{CN})_2]_3]$	av
C–C (ring), a	1.384	1.397	1.40	1.39
C–C(CN) ₂ , b	1.383	1.379	1.37	1.38
C–CN, c	1.432	1.427	1.42	1.43
C≡N, d	1.126	1.137	1.146	1.136
C ₃ ring, internal, e	60	60	60	60
C–C–C(CN) ₂ , f	150.7	150.0	150.0	150.2
C–C–CN, g	120.6	120.8	120.7	120.7
NC–C–CN, h	118.9	118.4	118.6	118.6
C–C≡N, i	177.9	178.0	177.7	177.9

Table IV. Positional Parameters and Their Estimated Standard Deviations for 1:1 Triclinic $[\text{Co}(\text{C}_5\text{Me}_5)_2][\text{C}_3[\text{C}(\text{CN})_2]_3]^{-}$

atom	x	y	z	$B_{\text{ISO}}, \text{Å}^2$
Co	0.1021 (1)	0.33662 (4)	0.67745 (6)	2.18 (2)
N21	0.3038 (9)	0.2901 (3)	0.3125 (4)	5.1 (1)
N22	0.0610 (8)	0.2567 (3)	0.0163 (4)	4.8 (1)
N28	0.4828 (8)	0.0477 (2)	0.3204 (3)	4.5 (1)
N29	0.4603 (8)	-0.2208 (2)	0.0341 (4)	5.2 (1)
N31	0.0288 (8)	0.0009 (4)	-0.2344 (4)	4.6 (1)
N32	0.2592 (8)	-0.2441 (2)	-0.2165 (4)	4.9 (2)
C1	-0.1533 (7)	0.2288 (3)	0.6988 (4)	3.6 (2)
C2	-0.136 (1)	0.3071 (4)	0.5726 (4)	4.8 (2)
C3	-0.1038 (9)	0.4033 (4)	0.6575 (5)	4.2 (2)
C4	-0.1081 (8)	0.3909 (3)	0.7450 (5)	4.2 (2)
C5	-0.1416 (9)	0.2818 (4)	0.7115 (4)	3.9 (2)
C6	-0.199 (1)	0.1146 (5)	0.5456 (7)	6.4 (2)
C7	-0.146 (1)	0.2844 (6)	0.4660 (5)	7.3 (2)
C8	-0.979 (1)	0.5091 (3)	0.6556 (7)	8.7 (3)
C9	-0.989 (1)	0.4758 (5)	0.5837 (6)	7.9 (2)
C10	-0.163 (1)	0.2313 (6)	0.7816 (5)	7.0 (2)
C11	0.3454 (7)	0.3986 (4)	0.6461 (4)	3.2 (1)
C12	0.3133 (8)	0.2848 (3)	0.6062 (4)	3.7 (2)
C13	0.3055 (8)	0.2655 (3)	0.6911 (4)	3.1 (1)
C14	0.3347 (7)	0.3603 (4)	0.7810 (4)	2.6 (1)
C15	0.3610 (9)	0.4428 (3)	0.7521 (4)	3.5 (1)
C16	0.368 (1)	0.4511 (4)	0.5826 (5)	6.5 (2)
C17	0.294 (1)	0.2072 (4)	0.4991 (5)	6.7 (2)
C18	0.284 (1)	0.1577 (3)	0.6848 (5)	5.4 (2)
C19	0.343 (1)	0.3746 (4)	0.8870 (5)	4.7 (2)
C20	0.401 (1)	0.5553 (4)	0.8227 (5)	5.2 (2)
C21	0.2679 (8)	0.2402 (3)	0.2263 (4)	3.2 (1)
C22	0.1335 (9)	0.2217 (4)	0.0603 (4)	3.2 (1)
C23	0.2170 (8)	0.1811 (4)	0.1188 (4)	2.9 (1)
C24	0.2477 (7)	0.0815 (3)	0.0697 (4)	2.8 (1)
C25	0.3119 (7)	0.0002 (4)	0.0733 (3)	2.0 (1)
C26	0.2372 (6)	-0.0073 (3)	-0.0206 (3)	2.5 (1)
C27	0.3883 (7)	-0.0428 (4)	0.1272 (4)	2.4 (1)
C28	0.4389 (7)	0.0090 (3)	0.2345 (4)	2.7 (1)
C29	0.4272 (8)	-0.1426 (3)	0.0750 (4)	3.3 (1)
C30	0.1924 (8)	-0.0639 (4)	-0.1241 (4)	3.0 (1)
C31	0.0998 (8)	-0.0280 (4)	-0.1862 (4)	3.0 (1)
C32	0.2323 (7)	-0.1642 (3)	-0.1746 (4)	3.1 (1)

(28) (a) Cromer, D. T.; Waber, J. T. *International Tables for X-Ray Crystallography*; The Kynoch Press: Birmingham, England, 1974; Vol. IV, Table 2.2B. (b) Ibers, J. A.; Hamilton, W. C. *Acta Crystallogr.* **1964**, *17*, 781. (c) Cromer, D. J. *International Tables for X-Ray Crystallography*; The Kynoch Press: Birmingham, England, 1974; Vol. IV, Table 2.3.1.

(29) (a) Cheng, C.; Reiff, W. M. *Inorg. Chem.* **1977**, *16*, 2092. (b) Miller, J. S.; Dixon, D. A.; Calabrese, J. C.; Vazquez, C.; Krusic, P. J.; Ward, M. D.; Wasserman, E.; Harlow, R. L. *J. Am. Chem. Soc.* **1990**, *112*, 381–398.

(30) Takachs, L.; Takachs, J.; Reiff, W. M.; Ramsden, J. D. *Rev. Sci. Instrum.* **1986**, *57*, 2605–2608.

(31) E.g.: Herbstein, F. H. *Perspect. Struct. Chem.* **1971**, *4*, 166–395. Shibaeva, R. P.; Atovmyan, L. O. *J. Struct. Chem.* **1972**, *13*, 514–531. Endres, H. In *Extended Linear Chain Complexes*; Miller, J. S., Ed.; Plenum Publishing Co.: New York, 1983; Vol. 3, p 263 and references therein.

$[\text{C}_3[\text{C}(\text{CN})_2]_3]^{-}$ anion has C_{2v} molecular symmetry (Figure 1a). The average chemically equivalent bond distances and angles are summarized in Table III. This structure was the most precise of those investigated. Therefore, the bond lengths and distances for this structure are considered the most reliable.

The solid possesses segregated chains of $S = 1/2$ cations and $S = 1/2$ anions. This motif has been previously observed for electron-transfer salts of this anion,^{23,32} and is quite common for

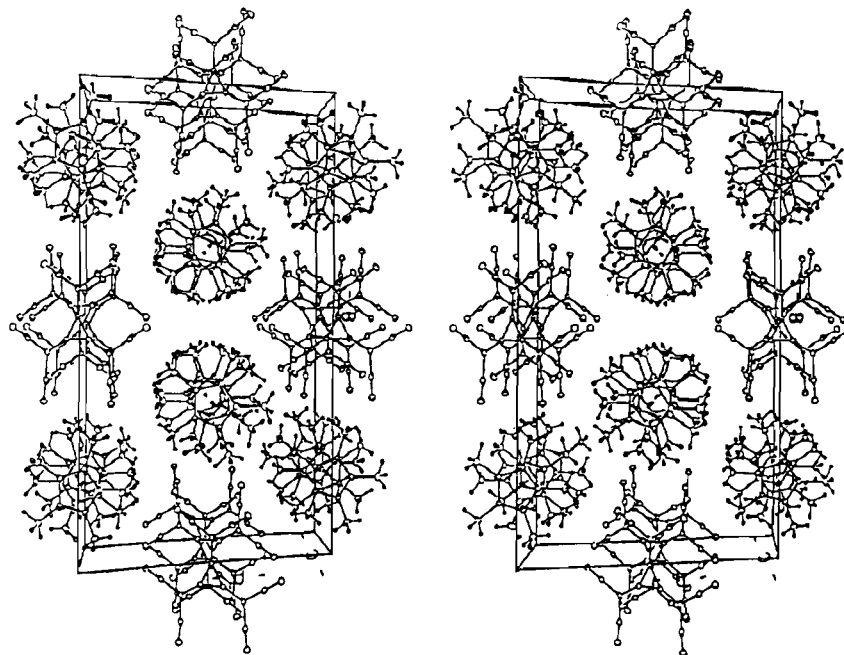


Figure 2. Stereoview of the unit cell of monoclinic $[Fe(C_6Me_5)_2]^+[C_3[C(CN)_2]_3]^{2-}$ down the c axis.

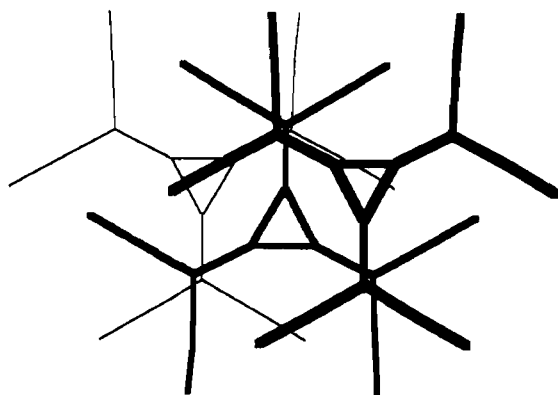


Figure 3. Overlap between three adjacent $[C_3[C(CN)_2]_3]^{2-}$ anions in monoclinic $[Fe(C_6Me_5)_2]^+[C_3[C(CN)_2]_3]^{2-}$.

equivalent bond distances and angles are summarized in Table III.

The solid-state structure reveals chains of $\{C_3[C(CN)_2]_3\}_2^{2-}$ dimers, i.e., $\cdots AA \cdots AA \cdots AA \cdots$ parallel to the b axis. The anions of the dimers are associated by overlap of the exocyclic carbon atoms. This motif is similar to that observed in the monoclinic phase (Figure 3) but with a slightly shorter *intradimer* interplanar separation of 3.154 Å. The $\{C_3[C(CN)_2]_3\}_2^{2-}$ dimer is located in the center of a triclinic unit cell and is surrounded by eight $[Fe(C_6Me_5)_2]^{2+}$ ions (Figure 5). The *interdimer* interplanar separation between $\{C_3[C(CN)_2]_3\}_2^{2-}$ dimers is only 2.880 Å. The actual intermolecular contact distances between dimers, however, are rather long since the neighboring anions are "slipped" as

depicted in Figure 6a. The closest *interdimer* contact (3.27 Å) is between a cyano nitrogen and one of the ring carbons.

The centroid of the $\{C_3[C(CN)_2]_3\}_2^{2-}$ dimer is located at the center of the unit cell, and the planes of the dimer unit are situated so as to form a dihedral angle of 137.45° with the arene rings of the cations. The observed orientation may be the result of charge-transfer interactions between the nitrogen atoms of the $\{C_3[C(CN)_2]_3\}_2^{2-}$ dimer with the mesitylene ring carbon atoms of the cations. One end of the anion is associated with a mesitylene ring with N2-C1 and N2-C2 distances of 3.31 (1) and 3.12 (1) Å, respectively, and a N6-C5 distance of 3.37 (1) Å (Figure 6). The other end exhibits close contacts with N3-C1 and N3-C6 distances of 3.48 and 3.14 Å, respectively (Figure 6b). Since the anions of the dimer are related by an inversion center, the two cations are symmetrically disposed about the $\{C_3[C(CN)_2]_3\}_2^{2-}$ dimer. The anions and cations thereby form unusual mixed-stack linear chains, i.e., $\cdots D^{2+}A_2^{2-}D^{2+}A_2^{2-} \cdots$, perpendicular to the a axis, forming a 153.4° angle with the anion chain axis. The C \cdots N intermolecular contacts and this type of motif are reminiscent of those recently reported for $[M(C_6Me_6)_2][(TCNQ)Cl_2]_2$ [(TCNQ)Cl₂ = 2,5-dichloro-7,7,8,8-tetracyano-*p*-quinodimethane] and $[M(C_6Me_6)_2][(TCNQ)F_4]_2$ (M = Fe, Ru) [(TCNQ)F₄ = perfluoro-7,7,8,8-tetracyano-*p*-quinodimethane].^{33,34} However, they differ significantly from the 1-D mixed-stack complexes $[M(C_6Me_6)_2]^{2+}[C_3[C(CN)_2]_3]^{2-}$ (M = Fe, Ru) in which the dianions are arranged in a face-to-face motif.³⁵

Notably, all of the well-characterized phases described here as well as those previously reported^{21,23} possess segregated chains of the $[C_3[C(CN)_2]_3]^{2-}$ anion. The apparent preference for this motif suggests favorable interactions between the $\{C_3[C(CN)_2]_3\}^{2-}$ anions.

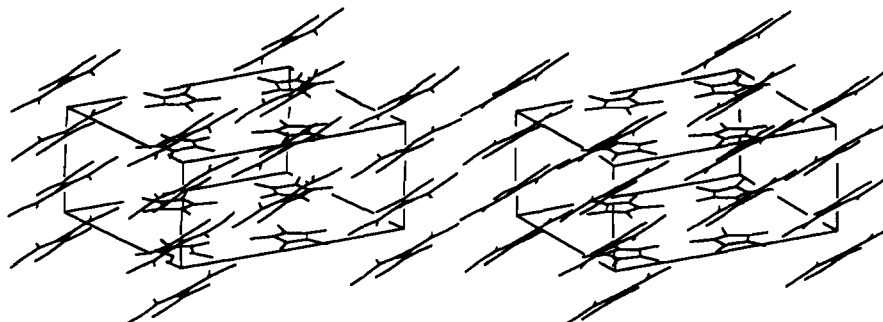


Figure 4. Stereoview of the unit cell of triclinic $[Co(C_6Me_5)_2]^+[C_3[C(CN)_2]_3]^{2-}$ down the c axis.

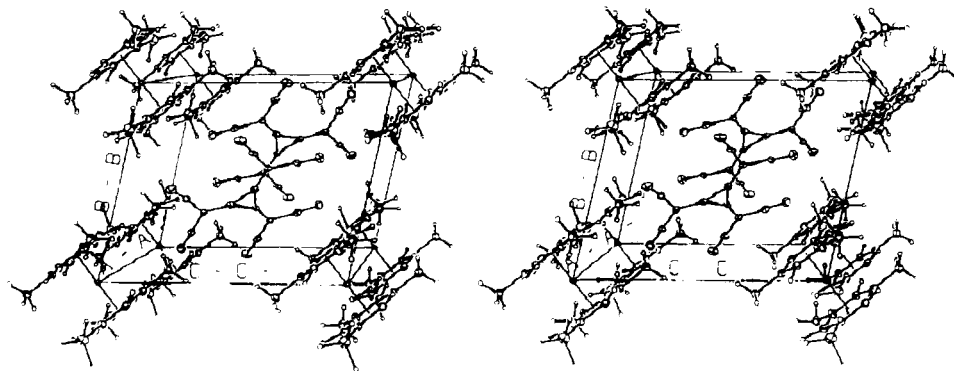
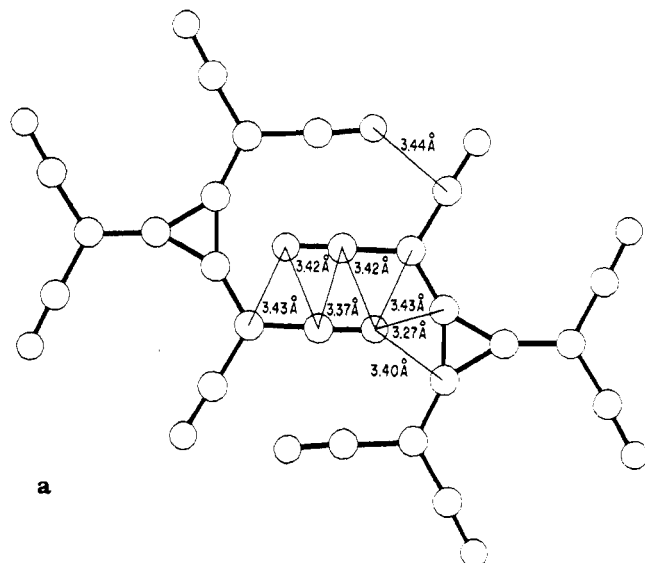
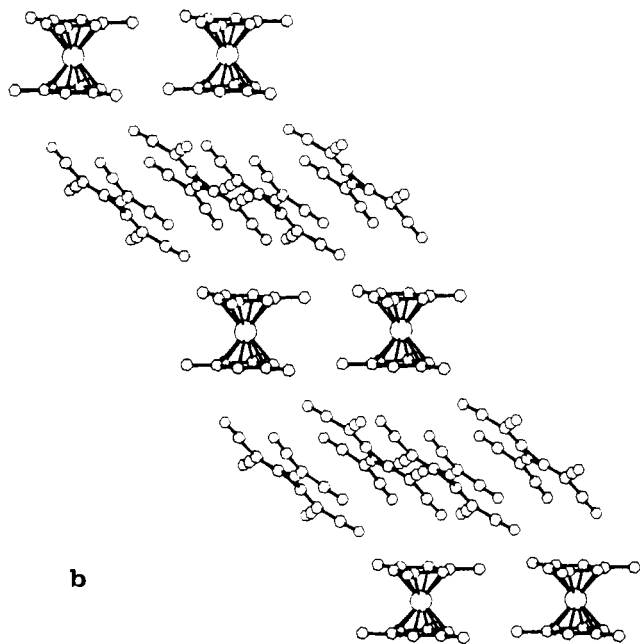


Figure 5. Stereoview of the unit cell of monoclinic $[\text{Fe}(\text{C}_6\text{H}_3\text{Me}_3)_2][\text{C}_3[\text{C}(\text{CN})_2]_3]_2$.



a



b

Figure 6. (a) Interaction between $[\text{C}_3[\text{C}(\text{CN})_2]_3]^{2-}$ anions in adjacent dimers. (b) orientation of $[\text{Fe}(\text{C}_6\text{H}_3\text{Me}_3)_2]^{2+}$ cations and $[\text{C}_3[\text{C}(\text{CN})_2]_3]^{2-}$ anions in $[\text{Fe}(\text{C}_6\text{H}_3\text{Me}_3)_2][\text{C}_3[\text{C}(\text{CN})_2]_3]_2$.

Mössbauer Spectra. Monoclinic $[\text{Fe}(\text{C}_5\text{Me}_5)_2]^{+}[C_3[\text{C}(\text{CN})_2]_3]^{2-}$. The zero-field ^{57}Fe Mössbauer spectra for monoclinic $[\text{Fe}(\text{C}_5\text{Me}_5)_2]^{+}[C_3[\text{C}(\text{CN})_2]_3]^{2-}$ as a function of temperature between 0.36 and 78 K are shown in Figure 7, while the Mössbauer parameters are presented in Table VI. The zero-field Mössbauer spectrum at ambient temperature for a velocity sweep of ± 4 mm/s

Table VI. Mössbauer Parameters for $[\text{Fe}(\text{C}_5\text{Me}_5)_2]^{+}[C_3[\text{C}(\text{CN})_2]_3]^{2-}$

<i>T</i> , K	isomer shift, (δ), mm/s	line width, (Γ), mm/s	internal field (H_n), kG
Monoclinic $[\text{Fe}(\text{C}_5\text{Me}_5)_2]^{+}[C_3[\text{C}(\text{CN})_2]_3]^{2-}$			
300	0.44	0.41	
78	0.47	0.89	
60	0.46	0.70	
50	0.45	0.61	
30	0.46		419
20	0.49		438
10	0.47		441
4.3	0.53		445
1.05	0.49		446
0.52	0.46	0.80 ^a	450
0.36	0.47	0.43 ^a	455
0.52 ^b	0.47		456
Triclinic $[\text{Fe}(\text{C}_5\text{Me}_5)_2]^{+}[C_3[\text{C}(\text{CN})_2]_3]^{2-}$			
48.7	0.61	0.66	
4.68	0.55	0.71 ^a	431

^a Average line width of six lines. ^b In the external field of 15.1 kG.

is fit to a singlet with isomer shift, δ , of 0.444 mm/s and line width, Γ , of 0.414 mm/s, values characteristic of the decamethylferrocenium cation.^{9,13,14,15b,16,36} This narrow singlet varies little between 100 and 300 K; however, gradual and unprecedentedly high-temperature broadening and hyperfine splitting below 100 K are clearly evident. This gradual increase in the intensity of the hyperfine splitting pattern with decreasing temperature is similar to that observed for the mixed-stack linear chain complex $[\text{Fe}(\text{C}_5\text{Me}_5)_2]^{+}[\text{DDQ}]^{2-}$ below 25 K,^{15b} is typical of slow paramagnetic relaxation as opposed to the onset of cooperative, extended 3-D magnetic ordering. There is no evidence of 3-D magnetic ordering or weak exchange from the susceptibility data for this temperature range (vide infra). The slow paramagnetic relaxation observed for the present complex in the zero-field is attributed in part to a small Zeeman splitting of the ground-state Kramers doublet of the $[\text{Fe}(\text{C}_5\text{Me}_5)_2]^{+}$ cation by dipolar fields arising from electron spin on the neighboring cations and anions. The Fe(III) cations are self-dilute with Fe...Fe separations of >8 Å, and this leads to long spin-spin relaxation times.³⁶ The decrease in temperature leads to longer spin-lattice relaxation times as the lower energy phonon states are populated. These effects along with the aforementioned Zeeman splitting induced via local dipolar fields results in unprecedented (relatively high temperature and in zero external applied field) slow relaxation in the $S = 1/2$ ground doublet of low-spin Fe(III).

The intensity from the central singlet corresponding to the rapidly relaxing paramagnetic phase persists to ~ 0.5 K at which the hyperfine splitting is still not fully resolved. At 0.36 K the spectrum exhibits the fully resolved characteristic six-line Zeeman pattern with narrow line widths (Figure 7, bottom). This *limiting spectrum* could arise from either slow paramagnetic relaxation combined with a 3-D magnetic ordering process as observed in

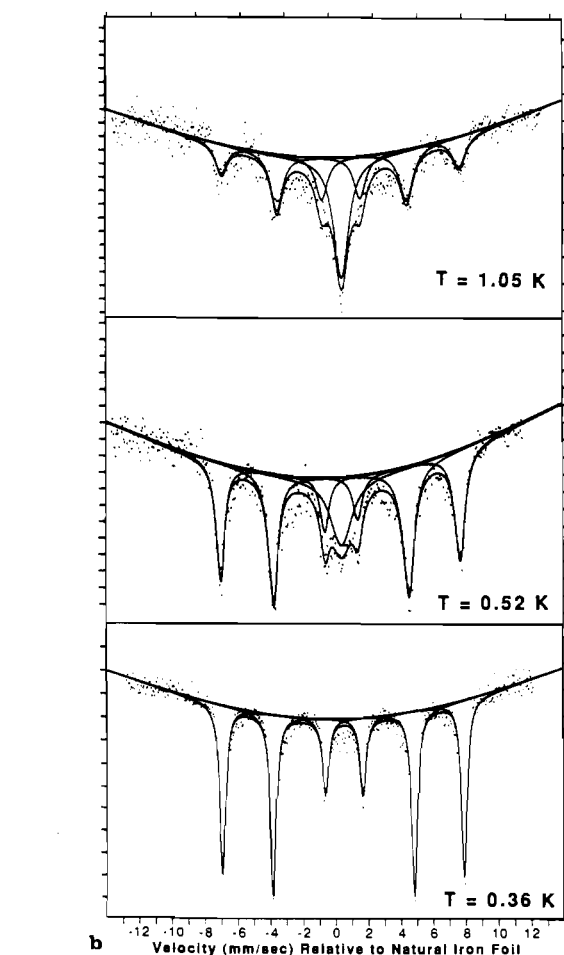
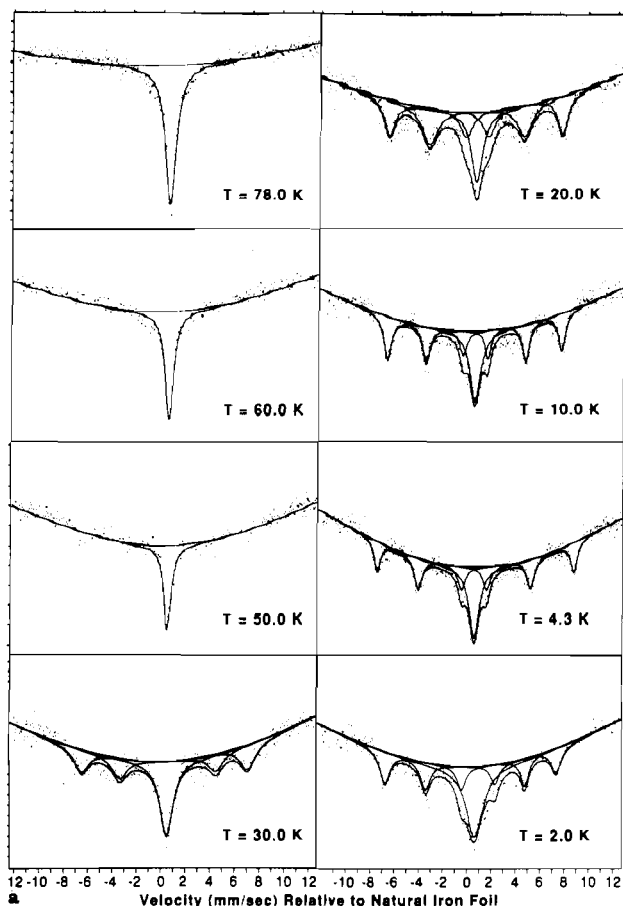


Figure 7. Zero-field temperature dependence of ^{57}Fe Mössbauer spectra for monoclinic $[\text{Fe}(\text{C}_5\text{Me}_5)_2]^{+}[\text{C}_3[\text{C}(\text{CN})_2]_3]^{-}$ between 2.0 and 78 K (a) and 0.36 and 1.05 K (b).

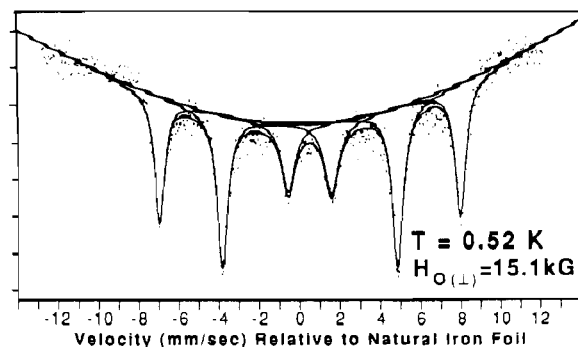


Figure 8. High-field dependence of ^{57}Fe Mössbauer spectra for monoclinic $[\text{Fe}(\text{C}_5\text{Me}_5)_2]^{+}[\text{C}_3[\text{C}(\text{CN})_2]_3]^{-}$ at 0.52 K.

$[\text{Fe}(\text{C}_5\text{Me}_5)_2]^{+}[\text{TCNQ}]^{-13}$ or more likely only slow paramagnetic relaxation in the limit of infinitely long relaxation time between the components of its ground Kramer's doublet as observed in the $[\text{DDQ}]^{-}$ salt.^{15b} Zero-field Mössbauer spectroscopy studies cannot readily distinguish these two situations as the limiting zero-field, low-temperature spectra corresponding to 3-D magnetic ordering processes are identical with those for slow relaxation.³⁷ To clarify this situation, susceptibility measurements at lower temperatures are necessary. The internal field at the limiting temperature of 0.32 K is 455 kG, which is comparable to that found for other $[\text{Fe}(\text{C}_5\text{Me}_5)_2]^{+}$ salts consisting of alternating cation-anion chains.

In a 5.2-kG applied field, the spectrum is only slightly changed relative to $H_0 = 0$ and intensity from the central peak is still evident. This strongly suggests that a significant fraction of the material is still in a rapidly relaxing paramagnetic state. In a transverse applied field of 15.1 kG (Figure 8), the material is nearly fully polarized such that it exhibits a hyperfine splitting intensity pattern of 2.2:2.6:1:1:2.6:2.2., i.e., approaching an intensity pattern of 3:4:1:1:4:3. This latter is precisely the intensity profile that one expects to induce via a transverse applied field ($H_0 \perp E_\gamma$) for either a paramagnetic or a ferromagnetically ordered species. The latter is, however, ruled out by the magnetic susceptibility and magnetization (vide infra).

Triclinic $[\text{Fe}(\text{C}_5\text{Me}_5)_2]^{+}[\text{C}_3[\text{C}(\text{CN})_2]_3]^{-}$. The ^{57}Fe Mössbauer spectra for the triclinic phase is essentially identical with that of the monoclinic phase, and the data are summarized in Table VI.

Magnetic Susceptibility. Monoclinic $[\text{Fe}(\text{C}_5\text{Me}_5)_2]^{+}[\text{C}_3[\text{C}(\text{CN})_2]_3]^{-}$. The temperature dependence of the reciprocal susceptibility and magnetic moment for the monoclinic phase in applied fields of 5.1–19.5 kG between 2.2 and 360 K can be fit to the Curie-Weiss expression, $\chi = C/(T - \Theta)$ (Figure 9). The observed Θ 's for five samples of differing crystallinity were -0.66 , -0.73 , -2.40 , -5.20 and -7.92 K and average -3.4 K, while the μ_{eff} values are 2.82, 2.82, 2.96, 3.08, and 3.21 μ_B and average 2.98 μ_B . The negative Θ value indicates antiferromagnetic coupling. The magnetic moment is significantly lower than those observed for radical anion salts of $[\text{Fe}(\text{C}_5\text{Me}_5)_2]^{+}$ with one spin on the cation and one spin on the anion,^{6,8,9,13,15,16} which are larger than expected due to the anisotropic g factor of the cation coupled with alignment of the sample in the magnetic field. For example, a value of 3.50 μ_B was reported for $[\text{Fe}(\text{C}_5\text{Me}_5)_2]^{+}[\text{DDQ}]^{-}$.^{15a} The observations here are consistent with free spin residing only on the cation; the $[\text{C}_3[\text{C}(\text{CN})_2]_3]^{2-}$ anions have short interanion separations of 3.22 Å, leading to antiferromagnetic coupling and a singlet ground state. On the basis of our previous experience with $[\text{Fe}(\text{C}_5\text{Me}_5)_2]^{+}$ salts, orientation of the sample in the magnetic field is expected. For the cation itself, the anticipated spin-only value isotropic moment is 2.20 μ_B based on $g_{\parallel} = 4.00$ and $g_{\perp} = 1.3$,³⁸ i.e., $\langle g \rangle = 2.54$. Perfect alignment of the crystal, neglecting an anion spin, along the C_5 axis would result in $\mu_{\text{eff}} = 3.46 \mu_B$. Thus, the observed moment appears to be consistent with some sample alignment with the field, orbital contributions to the moment, and diamagnetic anion chains.

(37) Vignall, J. W. G. *J. Chem. Phys.* **1968**, *44*, 2462.

(38) Duggan, D. M.; Hendrickson, D. N. *Inorg. Chem.* **1975**, *14*, 955–970.

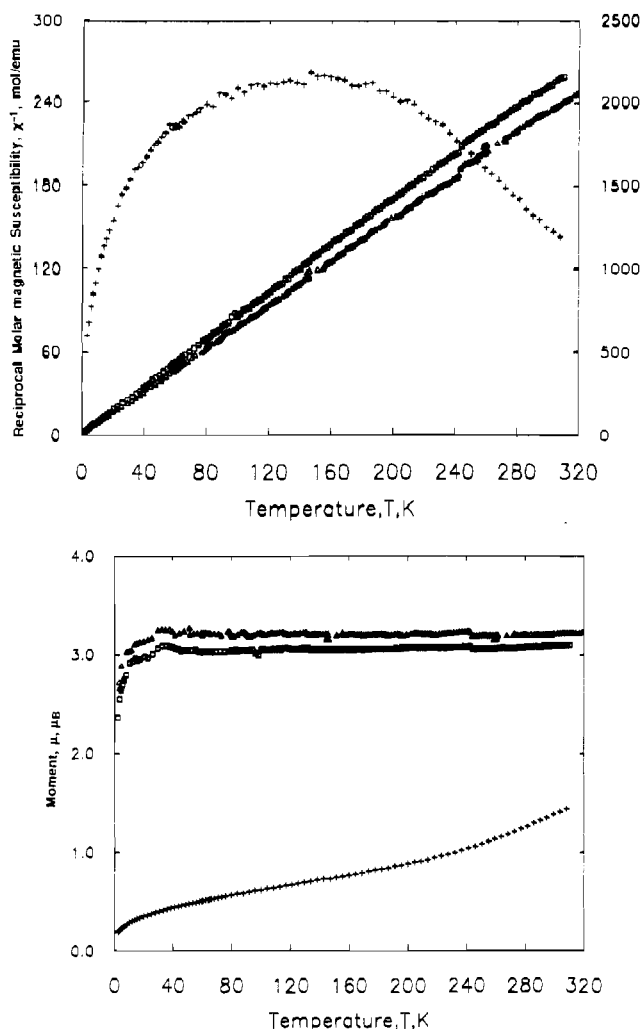


Figure 9. Reciprocal molar magnetic susceptibility, χ_M^{-1} , (top) and moment, μ_{eff} , (bottom) as a function of temperature for monoclinic (Δ) and triclinic (\square) $[\text{Fe}(\text{C}_3\text{Me}_5)_2]^{+}[\text{C}_3[\text{C}(\text{CN})_2]_3]^{-}$ and $[\text{Fe}(\text{C}_6\text{Me}_3\text{H}_3)_2]^{2+}[\text{C}_3[\text{C}(\text{CN})_2]_3]^{2-}$ (+).

To verify this claim, the magnetization as a function of applied field was obtained at 2 K by using a SQUID susceptometer for a random sample cooled in a zero applied magnetic field and analyzed in terms of the Brillouin function for $S = 1/2$ systems

$$M = \sum N g_i J \tanh(x_i)$$

where

$$x_i = \mu_i H / k_B T = g_i J H / k_B T$$

N is Avogadro's number, and g_i and μ_i refer to the Landé g factor and magnetic moment of each spin site i . The experimental data are plotted as a function of H vs T with two theoretical curves in Figure 10. The top theoretical curve assumes two spins per formula, i.e., one on the cation and the other on the anion, whereas the lower curve assumes spin only on $[\text{Fe}(\text{C}_3\text{Me}_5)_2]^{+}$. The experimental data fit the theoretical curve for spin only on the cation, especially in the small H vs T region where the intra- and intermolecular magnetic interactions are not significant and where the field-induced crystallite alignment effects are not important. The magnetization up to 20 kG shows that the extended magnetic interactions are not significant, and magnetic saturation is not achieved at 2.0 K.

The 1.6–60 K temperature variations of the molar susceptibility and magnetic moment at 10 different applied fields ranging from 1.6 to 5.1 kG are shown in Figure 11. As the temperature is decreased, the magnetic moment rises rapidly from a lower state ($\sim 2.8 \mu_B$) to a higher state ($\sim 3.5 \mu_B$) at ~ 4 K indicative of a field-induced phase transformation. The susceptibility exhibits little field dependence above and below ~ 4 K, implying that the higher moment state is not ferromagnetic (the susceptibility of

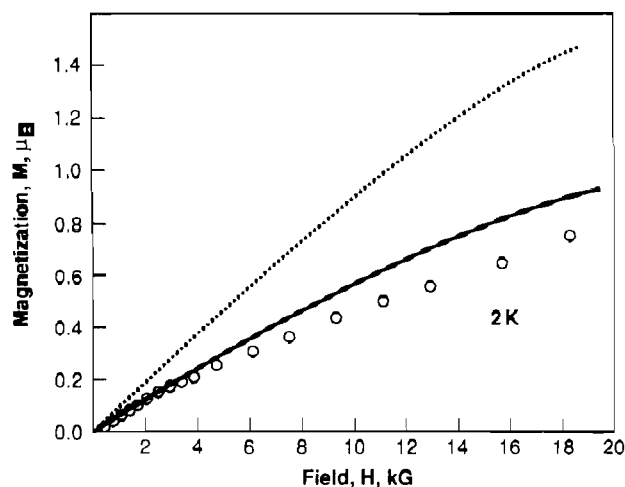


Figure 10. Magnetization as a function of field for monoclinic $[\text{Fe}(\text{C}_3\text{Me}_5)_2]^{+}[\text{C}_3[\text{C}(\text{CN})_2]_3]^{-}$ at 2 K.

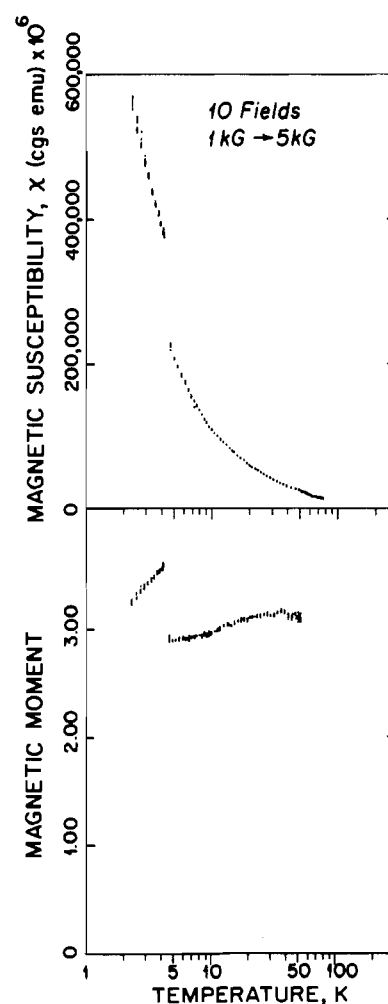


Figure 11. Molar magnetic susceptibility and magnetic moment as a function of temperature for monoclinic $[\text{Fe}(\text{C}_3\text{Me}_5)_2]^{+}[\text{C}_3[\text{C}(\text{CN})_2]_3]^{-}$ at 10 fields between 1.66 and 5.1 kG.

a ferromagnetic sample would decrease with increasing applied fields due to demagnetization effects as observed in $[\text{Fe}(\text{C}_3\text{Me}_5)_2]^{+}[\text{TCNE}]^{9-11}$ or $[\text{Fe}(\text{C}_3\text{Me}_5)_2]^{+}[\text{C}_4(\text{CN})_6]^{-}$.¹⁶

To confirm the possibility of a field-induced phase transformation at ~ 4 K, more sensitive, low-field measurements (< 400 G) were made on a SQUID magnetometer. The temperature dependence of susceptibility, reciprocal susceptibility, and magnetic moment for different applied fields (H_0) are plotted in Figure 12. The susceptibility exhibits a broad maximum at ~ 4 K at 30 G. The maximum shifts to lower temperatures between 100 and 200

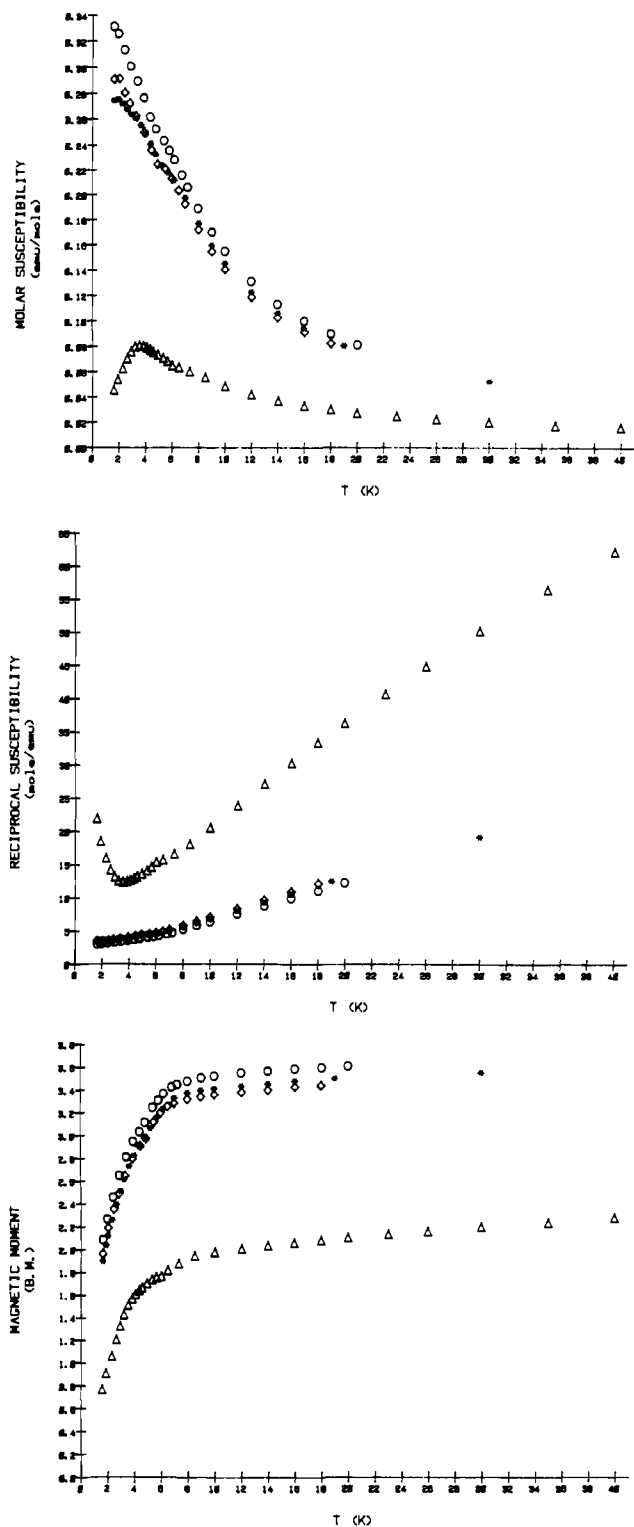


Figure 12. Molar magnetic susceptibility (a), reciprocal molar magnetic susceptibility (b), and magnetic moment (c) as a function of temperature for monoclinic $[Fe(C_5Me_5)_2]^{+}[C_3[C(CN)_2]_3]^{-}$ below 40 K: (O) $H = 400$ G; ($*$) $H = 200$ G; (\diamond) $H = 100$ G; (Δ) $H = 30$ G.

G and eventually disappears at 400 G. Below ~ 5 K, the magnetic moment gradually decreases and approaches $1.9 \mu_B$ at 1.6 K (Figure 12c), which is close to the spin-only value for one spin per formula weight.

The broad maximum observed in $\chi(T)$ for $H_0 \leq 100$ G undoubtedly results from a 1-D antiferromagnetic exchange interaction along the $[Fe(C_5Me_5)_2]^{+}$ chains. The susceptibility of isolated antiferromagnetically coupled pairs of magnetic sites can also exhibit similar broad maxima. Such antiferromagnetically coupled dimers, however, have an $S_{TOTAL} = 0$ ground state. In this case, magnetic hyperfine splitting of the Mössbauer resonances

would not be observed in contrast to our data. Also, weak antiferromagnetic interchain coupling of an assembly of ferromagnetic chains may yield a susceptibility with a broad maximum occurring at the transition temperature T_c . Thus, at T_c , the interchain coupling drives the system into long-range (3-D) ordering.³⁹ The $[Fe(C_5Me_5)_2]^{+}[TCNQ]^{-}$, $[Fe(C_5Me_5)_2]^{+}[TCNE]^{-}$,^{9,11} and $[Fe(C_5Me_5)_2]^{+}[C_4(CN)_6]^{+}$,^{16,11} salts have $\Theta = +3$, $+30$, and $+35$ K, respectively, indicating the dominance of ferromagnetic intrachain coupling. The monoclinic $[Fe(C_5Me_5)_2]^{+}[C_3[C(CN)_2]_3]^{-}$, however, exhibits a negative Θ , suggestive of antiferromagnetic intrachain coupling. Moreover, the field dependence of magnetization for $\{C_3[C(CN)_2]_3\}^{-}$ is not that expected for metamagnetic behavior. We therefore attribute the broad maximum in the susceptibility at 30 G to 1-D antiferromagnetic coupling along the cation chains, and propose that the anion chains are diamagnetic. Diamagnetism in $\{C_3[C(CN)_2]_3\}^{-}$ chains has ample precedence.^{21,23}

Bonner and Fisher⁴⁰ have determined the theoretical susceptibility behavior for a Heisenberg antiferromagnetic linear chain with $S = 1/2$ in which the following relations hold for $T_{max}(\chi)$ and χ_{max} :

$$k_B \chi T_{max} / |J| = 1.262$$

$$|J| \chi_{max} / N g^2 \mu_B^2 = 0.07346$$

From the experimental values of χT_{max} and χ_{max} , the intrachain coupling is estimated to be $J/k_B = -2.75$ K and $\langle g \rangle = 2.42$. The $\langle g \rangle$ value is in reasonable agreement with the observed g value for the $[Fe(C_5Me_5)_2]^{+}$ cation.³⁸ The small value of J indicates a very weak intrachain exchange interaction. Therefore, very small applied fields (≥ 100 G) are sufficient to decouple the very weak antiferromagnetic exchange interactions, inducing essentially complete transformation to a higher moment state.

Triclinic $[Fe(C_5Me_5)_2]^{+}[C_3[C(CN)_2]_3]^{-}$. The susceptibility of a powder sample was measured by using a Faraday apparatus between 2 and 300 K at a applied field of 4.8–19.5 kG (Figure 9). Simple Curie–Weiss behavior, $\Theta = -3.41$ K and $\mu_{eff} = 3.10 \mu_B$, was observed.

$[Fe(C_6Me_6H_3)_2]^{2+}[C_3[C(CN)_2]_3]^{2-}$. The structure has $\{C_3[C(CN)_2]_3\}^{2-}$ dimers with short interplanar spacings that would be expected to result in strong antiferromagnetic coupling between the $S = 1/2$ anions. Indeed, the magnetic susceptibility data between 2 and 340 K are consistent with a singlet ground state, but with a significant population of a triplet excited state at higher temperatures (Figure 9). In contrast to the case of decamethylferrocenium salts, the spin exchange coupling, J , could not be estimated from the moment plot as a maximum was not observed. The Bleaney–Bowers equation (eq 1)⁴¹ was used, however,

$$\chi = (N g^2 \mu_B^2 / k_B T) / [3 + \exp(J/k_B T)] \quad (1)$$

to determine J or, equivalently, the singlet–triplet energy. The value thus determined was 0.11 eV (1280 K, 890 cm^{-1} , 2.56 kcal/mol), which is typical of 1-D organic electron-transfer complexes.⁴²

The presence of a triplet excited state was also corroborated by EPR analysis. At room temperature, the EPR spectrum exhibited a singlet at $g = 2.00671$ (peak width at half-height = 3 G) and two pairs of weak features disposed symmetrically about the singlet ($g = 2.008$) (Figure 13). These features are attributed to thermally populated randomly oriented triplets.⁴³ Triplet fine structure is readily observed when the triplet population is small enough so that exchange broadening arising from triplet exciton collisions is not significant. Upon cooling, the intensity of the fine structure actually increased due to the increased ex-

(39) De Jongh, L. J.; Miedema, A. R. *Adv. Phys.* **1974**, *23*, 1.

(40) Bonner, J. C.; Fisher, M. E. *Phys. Rev.* **1964**, *A135*, 640.

(41) Carlin, R. L. *Magnetochemistry*; Springer-Verlag: New York, 1986; p 75 ff.

(42) Chesnut, D. B.; Arthur, P., Jr. *J. Chem. Phys.* **1962**, *36*, 2969. Chesnut, D. B.; Phillips, W. D. *J. Chem. Phys.* **1961**, *35*, 1002. Radhakrishnan, T. P.; Engen, D. V.; Zoos, Z. G. *J. Phys. Chem.* **1987**, *91*, 3273.

(43) Wasserman, E.; Snyder, L. C.; Yager, W. A. *J. Chem. Phys.* **1964**, *41*, 1763.

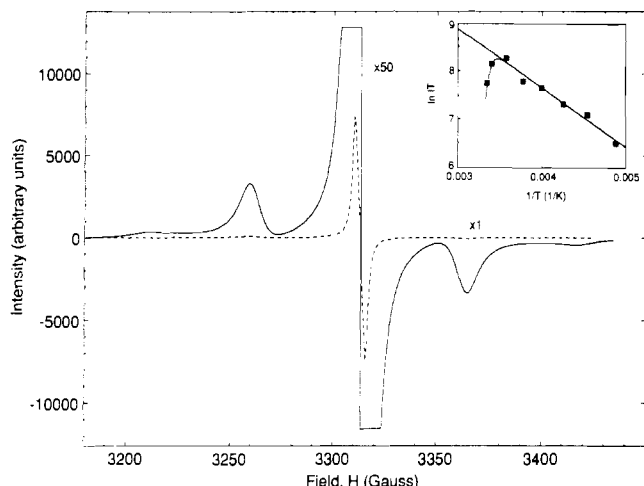


Figure 13. EPR spectra of $[\text{Fe}(\text{C}_6\text{Me}_3\text{H}_3)_2]^{2+}[\text{C}_3[\text{C}(\text{CN})_2]_3]_2^{2-}$ at 295 K. The lower spectra is identical with the upper, but is expanded by 25 \times to illustrate the triplet fine structure. The insert depicts the temperature dependence of the $\Delta m = \pm 2$ transition between 120 and 300 K.

change broadening even though the population of the triplet state decreased. Conversely, as the temperature is raised, spin exchange resulted in coalescence of the fine structure into a single sharp resonance, which is masked by the singlet associated with doublet impurities. The zero-field splitting parameter calculated from the fine structure splitting was $|D| = 104$ G. The lack of a third pair of lines suggested $|E| = 0$, in apparent contradiction with the less than orthorhombic symmetry of the $P\bar{1}$ space group. However, single-crystal experiments⁴⁴ indicated that $|E| = 3$ G. This small splitting is obscured in the powder spectrum by the broad triplet features (peak width at half-height ~ 15 G).

A weak half-field $\Delta m = \pm 2$ resonance at 1694 G was also observed at low temperature, where dipolar-induced mixing is evident from the presence of fine structure. The temperature dependence of the $\Delta m = \pm 2$ peak intensity corroborated the presence of a triplet excited state. The value of J can be determined from eq 2;^{45,46} for large values of $J/k_B T$ a plot of $\ln(I/T)$

$$I \propto 1/[T\{3 + \exp(J/k_B T)\}] \quad (2)$$

(44) Ward, M. D.; Morton, J. R.; Preston, K. *J. Chem. Phys.*, in press.

(45) Bijl, D.; Kainer, H.; Rose-Innes, A. C. *J. Chem. Phys.* **1959**, *30*, 765.

(46) Wertz, J. E.; Bolton, J. R. *Electron Spin Resonance, Elementary Theory and Practical Applications*; Chapman and Hall: New York, 1986; p 249.

vs $1/T$ can be used to estimate J with reasonable accuracy. The intensity of EPR resonances between 205 and 280 K indicated $J = 0.11$ eV; this is identical with that determined from the magnetic susceptibility. Above 300 K, the intensity drops sharply due to exchange broadening and the resulting reduction in dipolar-induced mixing. The agreement of the EPR and magnetic susceptibility data clearly shows that the triplet fine structure is due to a bulk species, which is tentatively attributed to the $[\text{C}_3[\text{C}(\text{CN})_2]_3]_2^{2-}$ dimers. A more detailed single-crystal EPR investigation will be reported independently.⁴⁴

Conclusion

Two polymorphs of $[\text{Fe}(\text{C}_5\text{Me}_5)_2]^{2+}[\text{C}_3[\text{C}(\text{CN})_2]_3]^{2-}$ have been isolated and structurally and magnetically characterized. The monoclinic polymorph possesses segregated cation and diamagnetic anion chains. This polymorph exhibits the Bonner–Fisher type of 1-D Heisenberg antiferromagnetic exchange interaction along the cation chain. The intrachain coupling, J/k_B , is -2.75 K. The interchain coupling, J'/k_B , is much smaller than J/k_B due to the intervening diamagnetic anion chain. Thus, 3-D magnetic ordering is not observed down to 0.32 K. To our knowledge, this is the first observation of such behavior for segregated chains of $[\text{Fe}(\text{C}_5\text{Me}_5)_2]^{2+}$. The triclinic polymorph possesses segregated radical cation and radical anion chains, and simple Curie–Weiss behavior is observed.

The 1:2 $[\text{Fe}(\text{C}_6\text{Me}_3\text{H}_3)_2]^{2+}[\text{C}_3[\text{C}(\text{CN})_2]_3]_2^{2-}$ salt possesses segregated chains of dication donors and dianion acceptors with a novel mixed-stack arrangement nearly normal to the segregated chains. Interactions between the cyanoanion nitrogen atoms and the cation's arene carbon atoms are implicated in the mixed stack chains. Mobile triplet excitons within these chains are observed and the triplet state is 0.11 eV (890 cm^{-1} ; 1280 K; 2.56 kcal/mol) above the ground state.

Acknowledgment. W.M.R. and J.H.Z. gratefully acknowledge support from the NSF DMR Solid State Chemistry Program, Grant No. 8313710. We appreciate the technical assistance provided by Carlos Vazquez, Daniel Wipf, William Marshall, Joseph C. Calabrese, Richard L. Harlow, R. Scott McLean, Ray Richardson, Edward Delawski, Fred Davidson, and Derrick Overall.

Supplementary Material Available: A summary of the crystallographic data (Table S1), atom-labeling diagrams, and tables of bond distances and angles, least-squares planes, and anisotropic thermal parameters for monoclinic $[\text{Fe}(\text{C}_5\text{Me}_5)_2]^{2+}[\text{C}_3[\text{C}(\text{CN})_2]_3]^{2-}$, triclinic $[\text{Co}(\text{C}_5\text{Me}_5)_2]^{2+}[\text{C}_3[\text{C}(\text{CN})_2]_3]^{2-}$, and $[\text{Fe}(\text{C}_6\text{Me}_3\text{H}_3)_2]^{2+}[\text{C}_3[\text{C}(\text{CN})_2]_3]_2^{2-}$ (28 pages); tables of calculated and observed structure factors (40 pages). Ordering information is given on any current masthead page.